THE ASTROPHYSICAL JOURNAL, 361:101–106, 1990 September 20

AN EXTREMELY CARBON-POOR PLANETARY NEBULA IN THE SMALL MAGELLANIC CLOUD

STEPHEN J. MEATHERINGHAM, STEPHEN P. MARAN, THEODORE P. STECHER, ANDREW G. MICHALITSIANOS, AND THEODORE R. GULL
Laboratory for Astronomy and Solar Physics, NASA/Goddard Space Flight Center
AND
LAWRENCE H. ALLER AND CHARLES D. KEYES
Department of Astronomy, University of California, Los Angeles
Received 1989 November 27; accepted 1990 March 20

ABSTRACT

New optical and ultraviolet observations of the type I planetary nebula SMP 28 in the Small Magellanic Cloud show that it is remarkably deficient in carbon (abundance less than 1/450th solar) and that the electron temperature is very high (25,200 K). The nebula may be so hot due to the lack of efficient cooling by carbon. Optical and UV data are well represented by a model in which the central star has temperature $T_* = 1.8 \times 10^5$ K and radius $R_* = 0.09\ R_\odot$. A nebular mass of 0.71 $M_\odot$ and a central star mass in the range 0.65–0.71 $M_\odot$ are inferred. Nitrogen is overabundant relative to oxygen by a factor of 1.57 compared to the mean abundances in SMC planetary nebulae (other type I objects excluded). It appears that SMC–SMP 28 has evolved from a massive progenitor, with main-sequence mass $M_{\rm init}$ greater than at least 5 $M_\odot$ and perhaps larger than 7 $M_\odot$, which underwent both second and third nuclear dredge-up, as well as very efficient hot bottom burning. These processes raised the surface abundances of He and N while depleting O and drastically reducing C. It appears that the study of type I nebulae can help constrain theoretical estimates of the efficiency of convective burning in the lower envelopes of intermediate-mass stars.

Subject headings: galaxies: Magellanic Clouds — nebulae: abundances — nebulae: planetary — stars: evolution

I. INTRODUCTION

Planetary nebulae (PNs) in the Magellanic Clouds furnish us with an excellent sample of objects with which to study the post–asymptotic giant branch stage of stellar evolution. Their distances are known to an accuracy of about 10%, and they are bright enough for detailed spectroscopy. The most serious current problem is a paucity of spatial information, most of the nebulae being less than 2″ in diameter. Nevertheless, there is a growing body of fundamental information on the kinematic, dynamic, and spectroscopic properties of these PNs (Aller *et al.* 1987; Barlow 1987; Dopita *et al.* 1985; Meatheringham 1988; Monk, Barlow, and Clegg 1988; Wood, Bessell, and Dopita 1986; Wood *et al.* 1987).

Spectroscopic studies of PNs are motivated by the possibility of elucidating the prenebular evolution of the progenitor star and thereby making useful tests of evolutionary models. Also, they provide insight into the role of PNs in the chemical enrichment of the interstellar medium. When photoionization modeling is applied to the spectroscopic data on a planetary nebula (PN), it is possible to generate a model that can account for a wide range of the observational data and which indirectly constrains the properties of the central star.

We report here on an optical and ultraviolet study of object 28 of Sanduleak, MacConnell, and Philip (1978) in the Small Magellanic Cloud, hereafter referred to as SMC–SMP 28. This nebula appeared from optical spectrophotometry to be a normal type I PN, characterized by enhanced abundances of He and N (Peimbert and Torres-Peimbert 1983) that result from second nuclear dredge-up in a progenitor star on the asymptotic giant branch (Becker and Iben 1979, 1980; Renzini and Voli 1981). As such, type I nebulae may derive from the most massive PN progenitors and are a relatively unusual and interesting class. SMC–SMP 28 was observed with the *International Ultraviolet Explorer* (*IUE*) as a target in our survey of optically selected type I PN in the Magellanic Clouds and was found to exhibit a surprising ultraviolet spectrum, with strong lines of ionized N and no detectable C emission. Here we present the currently available optical and ultraviolet data on this object (§§ II–IV) and interpret them in terms of current post–main-sequence evolutionary models for intermediate-mass stars in order to attempt to account for the chemical composition that we derive by ionization modeling.

II. OBSERVATIONS AND REDUCTION

a) Optical Spectra

Optical spectra were obtained on two separate occasions. First, a red spectrum from 4900 to 7100 Å was taken on the 3.9 m Anglo-Australian telescope (AAT) on the night of 1984 November 25. The detector used was the RGO spectrograph plus image photon counting system (Boksenberg 1972). The system setup was such that we achieved a spectral resolution of 6 Å. The range of line fluxes and detector dynamic range combined to saturate on the brightest nebular lines, and hence it was necessary to take a second exposure using neutral density filters. The second set of observations was on 1989 January 7, using the 2.3 m telescope at Siding Spring Observatory operated by the Australian National University. The detector was the double-beam spectrograph with photon counting array (Stapinski, Rodgers, and Ellis 1981). The spectrograph was operated with a dichroic to obtain simultaneous blue (3200–4700 Å) and red (4700–10000 Å) spectra, at a resolution of

10 Å. A second exposure was taken with the telescope defocused to prevent saturation of the brightest lines.

For both sets of optical observations, flat fields were obtained which enabled removal of pixel-to-pixel variations. The data were then converted to a linear wavelength scale using calibration arcs. The effects of the neutral density filters were removed from the observations made with the AAT. Finally, observations of standard stars with known flux distributions were used to remove large-scale structure across the detectors and calibrate the data in physical units.

Line intensities (relative to Hβ) were extracted by two methods. The first method was an automatic line finding and Gaussian fitting program. The second was a deconvolution option within the IRAF spectral plot program, and was used mainly to separate very close, or partially blended, lines. Both methods gave results that were identical within the expected errors.

The ratio of the brightest lines, the [O III] 4959,5007 Å doublet, as measured from the filtered (or defocused) spectrum is very close to the theoretical value, and hence we conclude that none of the optical lines was affected by saturation in the detector. The faintest lines measured are of the order of 3%–5% of Hβ, and it is these lines that have the largest uncertainties due to photon statistics. Lines observed near the ends of the detector formats have larger errors due to lower detector efficiencies. The two telescope/detector combinations gave very similar errors, and after combining the line measurements from both sets of spectra we estimated the errors as a function of intensity (relative to Hβ = 100) for the composite spectrum (Table 1A). Table 2 lists the final composite optical line intensities for SMC–SMP 28 from 3300 to 10000 Å.

The Hβ flux in SMC–SMP 28 is $(7.59 \pm 0.7) \times 10^{-14}$ ergs cm^2 s^{-1} (Meatheringham 1988). The tabulated observed line intensities in Table 2 can be scaled relative to Hβ to determine absolute reddened fluxes at Earth.

Two other sets of optical spectra for SMC–SMP 28 exist in the literature. Barlow (1987) obtained a blue spectrum from 3700 to 4400 Å at a resolution of ~1.6 Å. Monk, Barlow, and Clegg (1988) obtained a spectrum from 3600 to 7100 Å at a resolution of approximately 12 Å. On the whole, our line intensities agree well with their corresponding results. It should be noted that the Monk, Barlow, and Clegg spectrum was obtained with only a very short integration time (4 minutes), and hence the errors are quite large.

TABLE 1A

ESTIMATED ERRORS IN OPTICAL LINE INTENSITIES

INTENSITY (Hβ = 100)	WAVELENGTH RANGE (Å)			
	3300–3600	3600–7200	7200–8000	>8000
<3	>50%	>25%	>50%	>50%
3–6	50%	25%	50%	50%
6–15	25%	10%	25%	35%
15–30	25%	5%	10%	20%
>30	10%	<5%	<10%	20%

TABLE 1B

ESTIMATED ERRORS IN UV LINE INTENSITIES

Intensity (Hβ = 100)	Error
<30	75%
30–75	50%
75–100	30%
>100	15%

TABLE 2

LINE INTENSITIES

Wavelength (Å)	Identification	Observed Intensity (Hβ = 100)	Dereddened Intensity (Hβ = 100)
1241	N V	207	741
1404	O IV]	44	134
1487	N IV]	150	441
1550	C IV	<10	...
1576	[Ne V]	28	80
1640	He II	152	421
1663	O III]	30	84
1755	N III	191	532
1910	C III]	<10	...
3726	[O II]	15.3	17.7
3729	[O II]	10.7	12.4
3771	Hι	3.4	3.9
3798	Hθ	4.5	5.1
3835	Hη	8.2	9.3
3868	[Ne III]	60.7	68.8
3889	Hζ + He I	25.4	28.7
3967	[Ne III]	10.2	11.4
3970	Hϵ	15.2	17.0
4026	He I + He II	3.9	4.3
4068	[S II]	4.5	5.0
4101	Hδ	24.3	26.7
4340	Hγ	46.7	49.8
4363	[O III]	12.7	13.5
4686	He II	51.2	52.4
4712	He I + [Ar IV]	12.6	12.8
4740	[Ar IV]	6.4	6.5
4861	Hβ	100.0	100.0
4959	[O III]	85.2	84.4
5007	[O III]	286.7	282.3
5200	[N I]	3.8	3.7
5411	He II	7.2	6.8
5755	[N II]	7.7	7.0
5876	He I	19.6	17.7
6548	[N II]	58.1	49.6
6563	Hα	320.6	273.2
6584	[N II]	181.1	154.1
6678	He I	6.1	5.2
6725	[S II] + [S II]	12.6	10.6
7065	He I	18.9	15.6

b) Ultraviolet Spectra

SMC–SMP 28 was observed with the *IUE* on 1988 August 14 and 1989 March 27. Three exposures were taken totaling 33,780 s. The short-wavelength prime (SWP) camera was used in low-dispersion mode, giving spectral coverage from approximately 1200 to 2000 Å at a resolution of 6 Å. The angular size of SMP 28 is less than a 3″ *IUE* pixel; the spectrograph aperture has dimensions of 10″ × 20″.

Due to the faintness of the nebula the UV spectra were extracted using a Gaussian extraction method sensitive to the low number of counts in the observations (Urry and Reichert 1988). The three spectra were found to give consistent results and were weighted by exposure time and co-added to produce one 33,780 s net exposure (Fig. 1). Line intensities were measured for the UV emission lines. SMC–SMP 28 is virtually at the limit of *IUE*'s sensitivity and as such the associated errors are larger than for the optical lines. Table 2 lists the UV line intensities (relative to Hβ = 100), the errors of which are given in Table 1B. Neither C IV (1550 Å) nor C III] (1910 Å) were

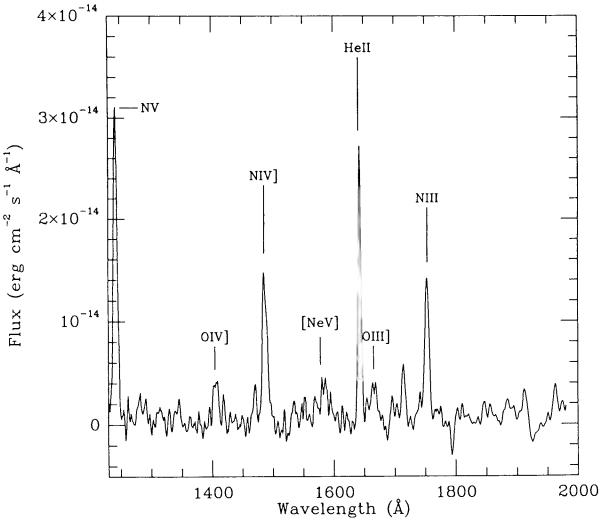

FIG. 1.—Flux-calibrated ultraviolet spectrum of SMC–SMP 28. Total exposure time 33,780 s. Note the absence of C IV (1550 Å) and C III] (1910 Å) emission.

detected with *IUE*, and we give upper limits for them. These carbon lines are usually among the most intense UV emission lines in this region of a PN spectrum.

RESULTS

a) *Nebular Diagnostics*

Both the electron temperature (T_e) and density (n_e) can be obtained from the usual [O III] and [O II] nebular line ratios,

$$\frac{I(4959)+I(5007)}{I(4363)} = 29.3\,\frac{I(3729)}{I(3727)} = 0.70\,. \qquad (1)$$

The [S II] 6717, 6731 Å lines were not resolved, and hence we cannot determine a [S II] electron density. Electron temperatures and densities were determined from five-level atomic models using the collision strengths of Pradhan (1976), together with the transition probabilities of Zeippen (1982). These give $T_e = 25{,}200$ K, and $n_e = 2160$ cm^{-3}. Each of these functions changes slowly enough as the other varies such that a small change makes virtually no difference to the derived value.

b) *Reddening*

It is important to obtain a good estimate of the reddening to SMC–SMP 28 in order to correct the observed line fluxes so they are useful in creating an accurate model of the nebula. Two methods were used.

Balmer Decrement.—Brocklehurst (1971) gives the case B hydrogen Balmer line intensities for various n_e and T_e. Interpolating to $n_e = 2160$ cm^{-3} and extrapolating to $T_e = 25{,}200$ K gives Hα:Hβ:Hγ:Hδ = 272:100:47.8:26.5. The extinction constant (c) is defined by $c = \log F_{\rm corr}(\mathrm{H}\beta) - \log F_{\rm obs}(\mathrm{H}\beta)$, where $F_{\rm corr}$ and $F_{\rm obs}$ are the true and observed Hβ fluxes, respectively. Line intensities other than Hβ are related by $I_{\rm corr}(\lambda) = I_{\rm obs}(\lambda)10^{cf(\lambda)}$, where $f(\lambda)$ is derived from Whitford (1958). Using these intensities we find $c(\mathrm{H}\alpha) = 0.23$, $c(\mathrm{H}\gamma) = 0.09$, and $c(\mathrm{H}\delta) = 0.21$. This gives an intensity weighted c(Balmer) = 0.21.

He II 1640/4686 Å *Ratio.*—We may use the He II line ratio in an analogous manner to the Balmer lines. Seaton (1978) calculated intensities of the UV He II recombination lines for various n_e and T_e. The appropriate value for SMC–SMP 28 is $I_{\rm corr} = I(1640)/I(4686) = 7.72$. We observe $I_{\rm obs} = 2.96$. Hutchings (1982) gives an ultraviolet extinction curve for the SMC, and together with the Seaton (1979) formulation we find $f(1640) = 2.136$, and hence, c(He II) = 0.19.

As the UV extinction curves for the galaxy and SMC differ in the ultraviolet we use the Hutchings (1982) formulation. However, in the visible it is sufficient to use the Whitford (1958) version. The values of c derived by the two methods are very close, and for simplicity we assume $c = 0.21$ in the remainder of this paper. We believe that the optical line intensities are more accurate, and that the difference between the two values of c implies only a very minor change in the fluxes of the UV lines, and virtually no change to optical fluxes. Table 2 lists the dereddened line intensities for all of the observed UV and optical lines. Monk, Barlow, and Clegg (1988) find $c(\mathrm{H}\alpha) = 0.16$, but they assumed a mean $T_e = 10{,}000$ K to determine the Balmer decrement even though they found $T_e = 24{,}600$ K.

IV. PHOTOIONIZATION MODELING

Given a set of dereddened emission-line fluxes it is logical to attempt to create a model system consisting of a star and nebula that reproduce them. In practice, detailed modeling is extremely difficult and has only been carried out for a few galactic PNs (e.g., NGC 7662 by Harrington *et al.* [1982], and IC 3918 by Clegg *et al.* [1987]). In the case of SMC–SMP 28 we need to make certain simplifying assumptions. For instance, we have no spatial information, and hence, the derived nebular density and temperature are mean values over the nebula. We have no information about the nebular shape, but type I planetaries are often seen to exhibit bipolar or filamentary structure, being optically thin in some directions, while still maintaining a high optical depth in others. This large range in optical thickness accounts for the high and low ionization lines seen side-by-side in type I nebulae. However, even with these uncertainties, we may still calculate a model that can tell much about the unobserved central star (mass, luminosity, size, etc.), as well as about the nebula.

The usual approach to modeling such a system is to use a photoionization code, working outward from the central star in discrete steps, and at each step calculating a new radiation field distribution, line emissivities, ionization fractions, etc. The final aim of the program is to successfully predict the observed line intensities. Many parameters must necessarily be input to the program, some are fixed, and others free to change. For instance, the basic atomic parameters are effectively fixed, while those describing the central star (stellar atmosphere, radius, temperature, surface gravity, metallicity, etc.), and nebula (size, chemical composition, density distribution, etc.) can be varied.

Nebular abundances can be determined in two ways. First, the observed line intensities of the observed ionization stages may be taken and corrected for missing ionization stages using ionization correction factors (ICFs) to determine total abundances of given elements. However, these ICFs are basically ad hoc rules, so some workers prefer to calculate ionization models with a set of initial elemental abundances that are varied until agreement with observations is obtained. In any case it is imperative to measure spectral lines from as many different ionization stages as possible to establish accurate abundances.

While many authors have calculated detailed model atmo-

spheres for the nuclei of PN (e.g., Hummer and Mihalas 1970, *a*, *b*; Cassinelli 1971; Kunasz, Hummer, and Mihalas 1975; Husfeld *et al.* 1984; Clegg and Middlemass 1987), none has created a sufficiently fine grid of models over a large enough range in stellar temperature and gravity to cover the region of the Hertzsprung-Russell diagram occupied by the planetary nebula nuclei (PNN). One is forced to interpolate within a set of atmospheres which is not difficult and presents few uncertainties; however, it is often necessary to compare results directly from different authors' atmospheres, and this does present problems. For instance, some of the available model atmospheres are plane parallel, others spherical; some are H/He atmospheres, others contain metal edges; some assume LTE, others non–LTE. The present lack of an adequate and coherent set of atmospheres may lead to appreciable errors in the PNN parameters determined from photoionization modeling.

For a complete description of the modeling procedure used in this paper see Aller *et al.* (1987), (§ III*b*). In brief, the models are fitted by adjusting the parameters until satisfactory agreement is reached with observed information (line intensities, electron temperature, Hβ flux, etc.) The basic atomic parameters (photoionization cross sections, recombination and charge exchange coefficients, collision strengths and transition probabilities) are those given in Mendoza (1983) and Aller (1984), and references therein.

The distance of the SMC is taken here to be 63.1 kpc (Conti, Garmany, and Massey 1984). The absolute Hβ flux of SMC–SMP 28 is taken from Meatheringham (1988) and corrected for our derived interstellar reddening ($c = 0.21$) to give $F(\mathrm{H}\beta) = 1.23 \times 10^{-13}$ ergs cm^{-2} s^{-1}. The stellar atmospheres used were the non–LTE hydrogen and helium models of Clegg and Middlemass (1987).

Preliminary investigations indicated that the central star must be quite hot. This was inferred from the very high nebular electron temperature, and the presence of appreciable emissions of high-excitation stages (e.g., [Ne V]). Another consequence of the high electron temperature is that the effect of electron collisions from the ground state to higher levels of hydrogen may become important (Aller 1984). If such collisional excitation is present it would modify the Balmer decrement, tending to steepen it unless the electron temperature were in excess of 35,000 K. On the other hand, the He II levels would not be affected by collisional effects. The fact that values of the extinction coefficient, *c*, obtained by methods using hydrogen and helium, agree so closely suggests that collisional effects on the hydrogen levels are not very important. Collisional excitation of hydrogen would decrease the theoretical electron temperature, and enhance the difference between our observations and predicted intensities.

The models were set up with spherical symmetry and consisted of a central star, surrounded by a low-density zone ($n_e = 10$ cm^{-3}), followed by the spherical shell of the nebula with constant electron density. The procedure followed enables the truncation of nebulae at less than the Strömgren radius, allowing for density-bounded nebulae, as well as photoionization-limited ones.

The best-fit model to our data is for a star of $T_* = 1.8 \times 10^5$ K and $\log g = 6.6$. The stellar radius is 0.09 $R_\odot$, with an ultraviolet luminosity of 5480 $L_\odot$. The inner radius of the nebula is 0.04 pc, and the model is truncated at 0.128 pc. By comparison the nebula would have to extend to 0.1540 pc to encompass the full Strömgren sphere. The predicted Hβ flux (1.379×10^{-13}) is only 11% higher than observed. The predicted electron temperature is 25,350 K, extremely close to the value derived from the [O III] nebular line ratio. Note that this electron temperature is near the maximum seen in PNs. It is most difficult to obtain such a high value in models without forcing the He II 4686 Å flux to a much higher value than observed. A satisfactory model could only be obtained here by significantly reducing the adopted stellar atmosphere flux shortward of 4 rydbergs (the He^+ ionization limit), an approach that has often been used in modeling PNs.

The nebular abundances relative to $\log N(\mathrm{H}) = 12.00$ from the successful model are given in Table 3. The overall metallicity is 0.05 solar. It is extremely difficult to give meaningful errors associated with the abundances for many reasons (for example, uncertainty in atomic constants). However, the main modeling errors are determined from the number and intensity of various lines of different ionization stages observed for a given element. The largest errors are going to be for both sulfur and argon due to the lack of strong lines. Also listed in Table 3 are solar abundances, and the mean abundance for SMC PNs (excluding type I nebulae, and low-excitation objects) as determined by Monk, Barlow, and Clegg (1988). Due to the large range in composition found for type I nebulae it is meaningless to define a "mean" type I abundance; instead each is more easily compared to an average non-type I nebula. The upper limit tabulated for the carbon abundance corresponds to the upper limit on the lines of C IV (1550 Å) and C III] (1910 Å). Helium and nitrogen are quite overabundant relative to other PNs in the SMC (by factors of 2.5 and 2.4, respectively). This is to be expected as the object is a type I PN. However, the helium abundance is high even for a type I nebula. For example, Monk, Barlow, and Clegg (1988) find He/H ratios of 0.1 and 0.141 for two type I PNs in the SMC, and Peimbert (1984) gives 0.15 for a sample of SMC PNs. Carbon has previously been seen to be underabundant in SMC H II regions compared to the solar value by a factor of 31 (Dufour, Shields, and Talbot 1982), but this PN exhibits a deficiency of over 450! Similarly, oxygen is depleted by a factor of about 10, compared with other PNs in the SMC.

We may also determine the nebular ionized mass from the known information. Meatheringham (1988) gives the nebular mass as a function of the density, Hβ flux, and helium abundance:

$$M_{\mathrm{neb}} = 4\pi D^2 F(\mathrm{H}\beta)(1 + 4y)m_{\mathrm{H}}/(\alpha_{\mathrm{eff}}\, h\nu n_e)\,, \qquad (2)$$

where D is the distance, $y = N(\mathrm{He})/N(\mathrm{H})$ the helium abun-

TABLE 3

LOGARITHMIC NEBULAR ABUNDANCES

Element	SMC–SMP 28	Solar[a] $\log N(\mathrm{H}) = 12$	Mean SMC PN[b]
He	11.32	11.00	10.92
C	<6	8.67	8.71[c]
N	7.81	7.99	7.44
O	7.24	8.92	8.26
Ne	7.00	8.05	7.36
S	5.89	7.23	7.00[c]
Ar	5.62	6.6	5.6

[a] C, N, O, abundances from Lambert 1978; others from Aller 1986.

[b] From Monk, Barlow, and Clegg 1988, excludes type I, very low excitation (VLE) and low excitation (LE) nebulae.

[c] From Aller and Keyes 1987, for a sample of approximately 100 Galactic PNs.

dance, and $\alpha_{\rm eff}$ is the effective recombination coefficient of hydrogen for the emission of Hβ photons of energy $h\nu$. Brocklehurst (1971) and Aller (1984) only list $\alpha_{\rm eff}$ up to T_e = 20,000 K, and so we extrapolate to T_e = 25,200 K, $\alpha_{\rm eff} = 1.4 \times 10^{-14}$ cm^3 s^{-1}. This gives $M_{\rm neb} = 0.73\ M_\odot$ for a completely filled sphere, filling factor $\epsilon = 1$. However, $\epsilon = 0.97$ for SMC–SMP 28 and $M_{\rm neb} = 0.71\ M_\odot$. Note that an error in the adopted extrapolation of $\alpha_{\rm eff}$ can lead to a large error in nebular mass.

V. DISCUSSION

Paczyński (1971) determined that the mass of the central star of a planetary nebula is related to its luminosity such that $M_{\rm PNN} = 1.7 \times 10^{-5}\ L_* + 0.52$ (in solar units). We can find L_* from the stellar radius and temperature, leading to an estimated core mass for SMC–SMP 28 of $M_{\rm PNN} = 0.65\ M_\odot$. However, the mass determined in this way is model-dependent. For instance, if we take the Wood and Faulkner (1986) evolutionary tracks (Fig. 2), the central star's mass is dependent on the phase relative to helium shell flashing at which the PN envelope is ejected. Using their tracks we find a central star mass in the range $0.65 < M_{\rm PNN} < 0.72\ M_\odot$. This uncertainty is the best that can be expected based on the present data. Irrespective of the exact evolutionary track, and mass, the central star of SMC–SMP 28 lies to the high mass, high luminosity side of the main body of other PNN on the H-R diagram (Fig. 2), lending weight to the suggestion that type I PNs originate from higher mass progenitors that evolve into higher mass central stars. The other points in Figure 2 are from Gathier and Pottasch (1989) for a sample of Galactic PNs with accurately known distances.

The low carbon and oxygen abundances may be very important in setting the nebular electron temperature. Carbon, nitrogen, and oxygen are all important cooling agents in a nebula through the process of collisional excitation of low-lying energy levels, and the effect of lowering their abundances will certainly cut the nebular cooling significantly.

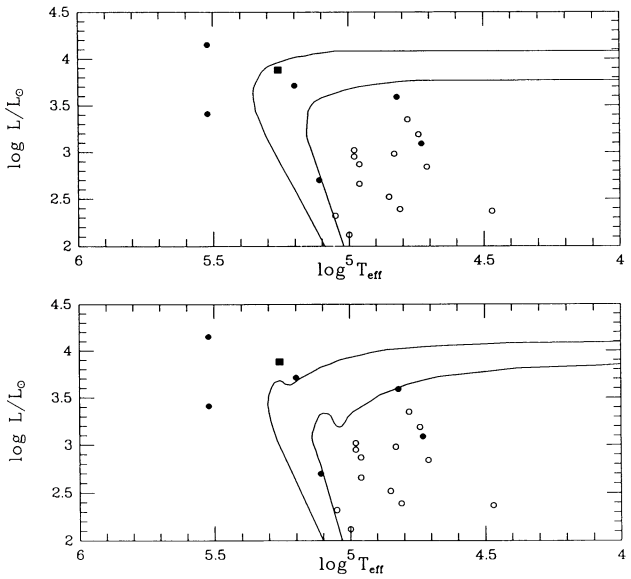

FIG. 2.—Evolutionary tracks from Wood and Faulkner (1986) for 0.60 and 0.70 $M_\odot$ central stars. The upper panel assumes PN ejection to occur midway between shell flashes, while the lower panel assumes ejection at rising surface luminosity during a shell flash. Shown is the position of SMC–SMP 28 (*filled square*). The other points are from Gathier and Pottasch (1989) for stars with accurately known distances and abundances (*filled circles*: larger He/H and/or N/O abundances; *open circles*: average abundances). SMC–SMP 28 lies to the high-luminosity, high-temperature side, together with the other type I nebulae.

The most interesting aspect of SMC–SMP 28 is its chemical composition. Although there is only an upper limit on the carbon abundance, the implications drawn for the post–main-sequence evolution of the progenitor star are robust. An instructive way to follow the earlier evolution of the star is to compare what we see with predictions of model calculations (Becker and Iben 1979, 1980; Renzini and Voli 1981). We are interested in seeing how much nuclear processing, if any, together with convective dredge-up is required to reproduce the observed abundances. Although no evolutionary models have been calculated for the abundance set derived here, it is still instructive to compare it with theory. We will use the Renzini and Voli (1981) results and note differences to the Becker and Iben (1979, 1980) papers when they occur.

There are three possible separate dredge-up phases during a star's post–main-sequence evolution according to Iben and Truran (1978). In the first dredge-up, the outer convective zone reaches down into regions where ^{12}C was partly converted to ^{13}C and ^{14}N during the main-sequence phase. Due to this, the surface abundances of ^{13}C and ^{14}N are raised, while ^{12}C is lowered. The ^{16}O abundance remains essentially unaltered. The second dredge-up occurs only in those stars with mass $M_{\rm init} > 3$–$5\ M_\odot$. In this phase, the convective envelope dips into the zone where hydrogen has been fully converted into helium, after the ignition of the helium burning shell, bringing up ^{14}N and He. Hence, the surface abundances of He and ^{14}N are enhanced, while carbon (^{12}C and ^{13}C) and ^{16}O are correspondingly reduced. This is the stage where it is believed that "typical" type I PN abundances are established. It appears impossible to get the final abundances found here simply through first and second dredge-up. Unless the star began its life with a very strange set of abundances (a conjecture for which there is no obvious support), it is not possible to lower the carbon surface abundance enough. There is a proposed third dredge-up process (Iben 1975) which would consist of a series of events occurring on the AGB. The base of the convective envelope dips inward after each helium shell flash, reaching a zone of incomplete helium burning, and bringing ^{4}He and ^{12}C to the surface. At first glance, although the third dredge-up raises the helium abundance as needed to satisfy our results, it also has the unwanted effect of increasing the carbon abundance. This problem can be eliminated by invoking nuclear burning at the base of the convective envelope itself, the so-called hot bottom burning (HBB) process (Becker and Iben 1980; Renzini and Voli 1981). During the AGB evolution, temperatures near the bottom of the envelope may become hot enough for significant amounts of CNO processing to take place. Products of this burning, ^{13}C and ^{14}N, are convected upward, at the expense of the surface abundances of ^{12}C and ^{16}O. However, the efficiency with which this process works is very sensitive to model assumptions and therefore predictions of resulting surface abundances are inexact. For example, the results of Renzini and Voli (1981) are in disagreement with Becker and Iben (1980) when HBB is taken into account. However, both sets of authors agree that the process is important in the more massive stars ($M_{\rm init} > 4$–$5\ M_\odot$). Unfortunately, an interesting test of the validity of this scenario, namely a search for ^{13}C around SMC–SMP 28, is not feasible.

What is the overall effect of the three dredge-up phases on

the final stellar atmospheric abundances? Can they be modified enough to produce the extreme type I PNs we see? The answer is probably yes. Renzini and Voli (1981) show the He/H ratio as a function of initial mass after each dredge-up episode, and with varying HBB efficiency. Although they do not produce He/H > 0.18, different initial stellar compositions could do so. It is clear, though, that third dredge-up will significantly help to raise the He/H level toward the value found in SMC–SMP 28. Note that the more efficient and the more active the HBB in a star, the greater the final He/H. Renzini and Voli (1981) also show log (C/O) and log (N/O) as a function of He/H, for various initial stellar masses, and with different amounts of HBB. The initial abundances are important, but will only have the effect of shifting the final He/H ratio. From their diagrams it is clear that without significant HBB the C/O ratio cannot be lowered to the upper limit found in this object, although the observed N/O may be obtainable. If we were simply to estimate an initial mass for the progenitor from their diagrams, it would seemingly exceed 5–7 $M_{\odot}$, whereas if we consider that the limit on C/O is the prevailing argument the inferred progenitor mass for SMC–SMP 28 must be close to the accepted upper limit on stars believed capable of forming PNs.

One other possible evolutionary scenario suggests itself, and that is a binary system. Iben and Tutakov (1985) present evolutionary calculations of close binaries with components having initial masses in the range $3 < M_{\rm init} < 12\ M_{\odot}$. However, none of their models seems to be able to reproduce correctly the set of abundances seen in SMC–SMP 28. The most common problem being that the surface helium abundances are much higher than we see. Hence, it appears that we can more easily reach the observed abundance set with a single star.

VI. CONCLUSIONS

SMC–SMP 28 appears to be a unique object, at the moment. The closest approximation among Galactic PN is possibly NGC 6537 (Fiebelman *et al.* 1985), in which nitrogen is enhanced and carbon and oxygen depleted, but by much smaller factors. SMC–SMP 28 is an extreme type I PN, which apparently has undergone all three stages of nuclear dredge-up, together with an appreciable amount of convective envelope burning (hot bottom burning). It is unclear from published post–main-sequence evolutionary calculations whether current models can reproduce the observed abundances seen in this object. However, the initial stellar composition would certainly play a part in modifying model predictions. SMC–SMP 28 may prove useful theoretically in further evaluating the role of hot bottom burning during the AGB phase.

We would like to acknowledge the financial support of the NASA *IUE Observatory* at Goddard Space Flight Center. S. J. M. also acknowledges support through a NRC Research Associateship.

REFERENCES

Aller, L. H. 1984, *Physics of Thermal Gaseous Nebulae* (Dordrecht: Reidel).
———. 1986, in *Spectroscopy of Astrophysical Plasmas*, ed. A. Dalgarno and D. Layzer (Cambridge: Cambridge University Press).
Aller, L. H., and Keyes, C. D. 1987, *Ap. J. Suppl.*, **65**, 405.
Aller, L. H., Keyes, C. D., Maran, S. P., Gull, T. R., Michalitsianos, A. G., and Stecher, T. P. 1987, *Ap. J.*, **320**, 159.
Barlow, M. J. 1987, *M.N.R.A.S.*, **227**, 161.
Becker, S. A., and Iben, I., Jr. 1979, *Ap. J.*, **232**, 831.
———. 1980, *Ap. J.*, **237**, 111.
Boksenberg, A. 1972, in *Proc. ESO/CERN conf. on Auxiliary Instrumentation for Large Telescope*, ed. S. Lansten and A. Reiz (Geneva: ESO/CERN), p. 295.
Brocklehurst, M. 1971, *M.N.R.A.S.*, **153**, 471.
Cassinelli, J. P. 1971, *Ap. J.*, **165**, 265.
Clegg, R. E. S., and Middlemass, D. 1987, *M.N.R.A.S.*, **228**, 759.
Clegg, R. E. S., Harrington, J. P., Barlow, M. J., and Walsh, J. R. 1987, *Ap. J.*, **314**, 575.
Conti, P. S., Garmany, C. D., and Massey, P. 1984, *Bull. AAS*, **16**, 948.
Dopita, M. A., Ford, H. C., Lawrence, C. J., and Webster, B. L. 1985, *Ap. J.*, **296**, 390.
Dufour, R. J., Shields, G. A., and Talbot, R. J., Jr. 1982, *Ap. J.*, **252**, 461.
Feibelman, W., Aller, L. H., Keyes, C. D., and Czyzak, S. J. 1985, *Proc. Natl. Acad. Sci. USA*, **82**, 2202.
Gathier, R., and Pottasch, S. R. 1989, *Astr. Ap.*, **209**, 369.
Harrington, J. P., Seaton, M. J., Adams, S., and Lutz, J. H. 1982, *M.N.R.A.S.*, **199**, 517.
Hummer, D. C., and Mihalas, D. 1970*a*, *M.N.R.A.S.*, **147**, 339.
———. 1970*b*, *J.I.L.A. Rept.*, no. 101.
Husfeld, R., Kudritski, R. F., Simon, K. P., and Clegg, R. E. S. 1984, *Astr. Ap.*, **134**, 139.
Hutchings, J. B. 1982, *Ap. J.*, **255**, 70.
Iben, I., Jr. 1975, *Ap. J.*, **196**, 525.
Iben, I., Jr., and Truran, J. W. 1978, *Ap. J.*, **220**, 980.
Iben, I., Jr., and Tutakov, A. V. 1985, *Ap. J. Suppl.*, **58**, 661.
Lambert, D. L. 1978, *M.N.R.A.S.*, **182**, 249.
Kunasz, P. B., Hummer, D. G., and Mihalas, D. 1975, *Ap. J.*, **203**, 92.
Meatheringham, S. J. 1988, Ph.D. Thesis, Australian National University, Canberra.
Mendoza, C. 1983, *IAU Symposium 103, Planetary Nebulae*, ed. D. Flower (Dordrecht: Reidel), p. 143.
Monk, D. J., Barlow, M. J., and Clegg, R. E. S. 1988, *M.N.R.A.S.*, **234**, 583.
Paczyński, B. 1971, *Acta. Astr.*, **21**, 417.
Peimbert, M. 1984, in *IAU Symposium 108, Structure and Evolution of the Magellanic Clouds*, ed. S. van den Bergh and K. S. de Boer (Dordrecht: Reidel), p. 363.
Peimbert, M., and Torres-Peimbert, S. 1983, *IAU Symposium 103, Planetary Nebulae*, ed. D. Flower (Dordrecht: Reidel), p. 233.
Pradhan, A. K. 1976, *M.N.R.A.S.*, **177**, 31.
Renzini, A., and Voli, M. 1981, *Astr. Ap.*, **94**, 175.
Sanduleak, N., MacConnell, D. J., and Philip, A. G. D. 1978, *Pub. A.S.P.*, **90**, 621.
Seaton, M. J. 1978, *M.N.R.A.S.*, **185**, 5P.
———. 1979, *M.N.R.A.S.*, **187**, 73P.
Stapinski, T. E., Rodgers, A. W., and Ellis, M. J. 1981, *Pub. A.S.P.*, **93**, 242.
Urry, M., and Reichert, G. 1988, *IUE NASA Newsletter*, No. **34**, 95.
Whitford, A. E. 1958, *A.J.*, **63**, 201.
Wood, P. R., Bessell, M. S., and Dopita, M. A. 1986, *Ap. J.*, **311**, 632.
Wood, P. R., and Faulkner, D. J. 1986, *Ap. J.*, **307**, 659.
Wood, P. R., Meatheringham, S. J., Dopita, M. A., and Morgan, D. H. 1987, *Ap. J.*, **320**, 178.
Zeippen, C. J. 1982, *M.N.R.A.S.*, **198**, 111.

THEODORE R. GULL, STEPHEN P. MARAN, STEPHEN J. MEATHERINGHAM. ANDREW G. MICHALITSIANOS, and THEODORE P. STECHER: Laboratory for Astronomy and Solar Physics, NASA/Goddard Space Flight Center, Code 680, Greenbelt, MD 20771

LAWRENCE H. ALLER and CHARLES D. KEYES: Department of Astronomy, University of California, Los Angeles, CA 90024